



Article

Optimization Model for Mine Backfill Scheduling Under Multi-Resource Constraints

Yuhang Liu ^{1,2} , Guoqing Li ^{1,*}, Jie Hou ¹ , Chunchao Fan ^{1,3}, Chuan Tong ^{1,3} and Panzhi Wang ³¹ School of Civil and Resource Engineering, University of Science and Technology Beijing, Beijing 100083, China² Department of Civil and Environmental Engineering, National University of Singapore, Singapore 119077, Singapore³ Jiaojia Gold Mine, Shandong Gold Mining (Laizhou) Company Limited, Yantai 261441, China

* Correspondence: qqlee@ustb.edu.cn

Abstract: Addressing the resource constraints, such as manpower and equipment, faced by mine backfilling operations, this study proposed an optimization model for backfill scheduling based on the Resource-Constrained Project Scheduling Problem (RCPSp). The model considered backfilling's multi-process, multi-task, and multi-resource characteristics, aiming to minimize total delay time. Constraints included operational limits, resource requirements, and availability. The goal was to determine optimal resource configurations for each stope's backfilling steps. A heuristic genetic algorithm (GA) was employed for solution. To handle equipment unavailability, a new encoding/decoding algorithm ensured resource availability and continuous operations. Case verification using real mine data highlights the advantages of the model, showing a 20.6% decrease in completion time, an 8 percentage point improvement in resource utilization, and a 47.4% reduction in overall backfilling delay time compared to traditional methods. This work provides a reference for backfilling scheduling in similar mines and promotes intelligent mining practices.

Keywords: RCPSp; mine backfilling; GA; scheduling optimization; intelligent mine



Citation: Liu, Y.; Li, G.; Hou, J.; Fan, C.; Tong, C.; Wang, P. Optimization Model for Mine Backfill Scheduling Under Multi-Resource Constraints.

Minerals **2024**, *14*, 1183. <https://doi.org/10.3390/min14121183>

Academic Editor: Bekir Genc

Received: 31 October 2024

Revised: 18 November 2024

Accepted: 19 November 2024

Published: 21 November 2024



Copyright: © 2024 by the authors. Licensee MDPI, Basel, Switzerland. This article is an open access article distributed under the terms and conditions of the Creative Commons Attribution (CC BY) license (<https://creativecommons.org/licenses/by/4.0/>).

1. Introduction

Backfilling allows for substantial disposal of mine waste into stopes, contributing significantly to safety, environmental protection, cost efficiency, and operational effectiveness [1–4]. As a crucial method for achieving green mining, zero-tailing operations, and sustainable resource extraction, backfill mining is progressively becoming the preferred practice in underground mining [5–8].

The operational efficiency of backfill mining largely depends on the coordinated management of multiple stopes, production stages, and resource allocations. Current scheduling and management techniques are typically inflexible, leading to lower resource utilization and production efficiency. Mines employing the backfill mining method handle several backfill tasks in numerous stopes on monthly and weekly schedules [9–11], with each stope requiring several sequential backfill steps involving multiple resources [12]. The backfill scheduling problem is characterized by high flexibility, allowing each stage to select among various parallel resources [13]. Enhancing backfill efficiency requires optimized resource coordination across projects, stages, and constraints. However, the core resource—the sand silo—is commonly managed in an “one operational, one standby” configuration, which imposes a rigid and inefficient framework.

In the era of Mining 4.0 and the development of intelligent mines, significant advances in backfill technologies have been achieved worldwide [14]. Increased investment has led to improved automation, enabling real-time adjustments of slurry concentration and composition as well as centralized control of material feeding, slurry mixing, and transportation processes [15–17]. Nonetheless, substantial opportunities remain to enhance

the allocation of key resources, such as manpower, equipment, and materials, to further optimize backfill operations.

These challenges are fundamentally optimization problems. Applying advanced scheduling optimization tools to backfill operations presents a promising research direction. Optimized workflows enhance control over the entire production process [18,19], aligning production with higher-level schedules and facilitating efficient resource allocation and task management.

A substantial body of research in production scheduling optimization, particularly in the manufacturing sector, centers on the Job Shop Scheduling Problem (JSP) [20]. The JSP, a foundational challenge in production scheduling, was introduced by Johnson in 1954 [21]. Later, in 1990, Bruker and Schlie [22] expanded the JSP to the Flexible Job Shop Scheduling Problem (FJSP), broadening equipment options from single to multiple machines, which enhanced flexibility and complexity, thus extending its applicability. Gong [23] further incorporated workforce flexibility into the FJSP framework, enabling improved human resource allocation. Key optimization metrics in FJSP include makespan, delivery delays, machine load, and energy consumption [24–26]. Additionally, preliminary studies have explored the application of these scheduling principles to mine backfill operations [27,28].

In model construction, certain assumptions are typically applied, with most models presuming continuous availability of manpower, materials, and equipment. However, real-world production environments are dynamic, complex, and subject to uncertainty, with frequent instances of equipment unavailability [29–32]. The Resource-Constrained Project Scheduling Problem (RCPSP), first introduced by Johnson and Russell in 1967 [33], addresses resource availability limitations by optimizing project planning and scheduling under resource constraints. RCPSP is widely used to optimize scheduling in vehicle fleets and production lines. In backfill operations, limitations stem from factors such as manpower constraints, equipment reliability issues, and unavailability due to sand silo loading and slurry preparation requirements, as well as equipment occupancy. Adapting RCPSP to the backfill context enables rational scheduling of backfill tasks according to equipment status, facilitating planned maintenance, optimizing timing for sand loading and unloading, and reducing extended delays.

In summary, while the adoption of backfill mining continues to expand, challenges related to rigid resource management and suboptimal utilization persist. Although automation and centralized control have advanced as part of intelligent mining development, these improvements have yet to fully inform scheduling decision-making. To address these issues, this study integrates resource constraints into a backfill scheduling optimization model, accounting for task parallelism and complex workflows. By systematically scheduling tasks with respect to both time and resource allocation, the model aims to fulfill target objectives while maximizing resource utilization.

The methodology of this study includes: first, identifying resource requirements for each backfill step and determining possible instances of resource unavailability; next, establishing model assumptions, defining input and output data, and setting model parameters, objectives, and constraints; subsequently, developing an algorithmic solution; and finally, validating the model and algorithm using actual mine data and analyzing scheduling results to evaluate the model's effectiveness.

2. Constraint Analysis

Backfill resources are categorized into three types: manpower, equipment, and materials. Among these, materials include tailings and cementitious components. Metal mines generate substantial amounts of tailings daily from mineral processing, with less than half typically allocated for backfilling under normal conditions [34]. The supply of cementitious materials is highly accessible, ensuring an adequate supply at any given time. Therefore, this study does not consider constraints on material resources.

Both manpower and equipment resources face limitations in production. The number of stopes that a backfill team can service simultaneously is capped, requiring the model to account for constraints on manpower occupancy.

Equipment encompasses various machinery used in backfilling operations. Equipment reliability is a critical factor for resource availability. Maintenance needs or equipment malfunctions can lead to unavailability and delays in tasks. Reliability degradation of key equipment components can impact the quality, speed, or energy consumption of backfilling. Therefore, the primary resource constraints in backfill operations include occupancy constraints, sandloading constraints, and reliability constraints.

2.1. Equipment Reliability Constraints

Analyzing equipment reliability allows for the quantification of its capability to perform designated functions, enabling the development of preventive maintenance plans. This approach also optimizes the allocation of available resources, ensuring the smooth progression of backfill operations.

If the failure behavior of backfill equipment follows a Weibull distribution, its probability density function is given by Equation (1), where t denotes the equipment’s service age, and β , η and r are the shape, scale, and location parameters. These parameters influence the curve’s shape, horizontal displacement, and scale. The cumulative distribution function (unreliability function) and reliability function are provided in Equations (2) and (3), respectively.

$$f(t) = \frac{\beta}{\eta} \left(\frac{t-r}{\eta} \right)^{\beta-1} e^{-\left(\frac{t-r}{\eta}\right)^\beta} \tag{1}$$

$$F(t) = \int_0^t f(t)dt = 1 - e^{-\left(\frac{t-r}{\eta}\right)^\beta} \tag{2}$$

$$R(t) = 1 - F(t) = e^{-\left(\frac{t-r}{\eta}\right)^\beta} \tag{3}$$

When $\beta < 1$, $\beta = 1$ and $\beta > 1$, these values respectively describe the early failure phase, random failure phase, and wear-out phase of the equipment, corresponding to the left, bottom, and right segments of the failure probability density curve, also known as the bathtub curve. The parameter η represents the characteristic life of the equipment, while $r > 0$ indicates the time at which failures begin to occur, representing the minimum service age.

Figure 1 illustrates the reliability variation of backfill equipment, where R represents equipment reliability. Equipment reliability decreases with increasing service age. Prior to each backfill task, the system evaluates whether the equipment’s reliability at the task’s completion would fall below the critical threshold RT . If the predicted reliability is below RT , maintenance is initiated. Complete maintenance restores the equipment to its original condition (“as good as new”), while partial maintenance improves reliability to an initial level, R^{ini} .

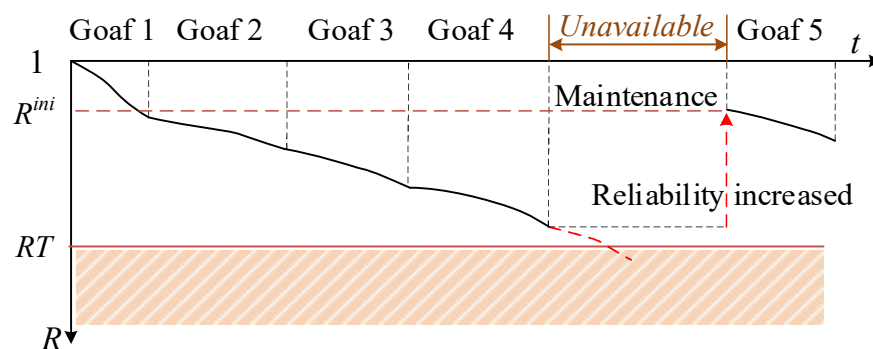


Figure 1. Schematic Diagram of Equipment Reliability and Availability.

2.2. Characteristics of Sand Silo Feeding and Slurry Preparation

The sand silo, a core component of the backfill system, thickens low-concentration tailings (about 20%, mass concentration) from the processing plant to a high concentration (around 80%, mass concentration) for use in mine backfilling after activation and slurry preparation [35].

Apart from reliability-related failures, the sand silo is also unavailable for slurry preparation at certain times due to its operational characteristics. Before discharging slurry, the silo must first undergo feeding and settling processes, during which it cannot support any backfilling operations. This is the primary reason mines adopt a “one operational, one standby” mode.

The sand silo feeding and settling process is illustrated in Figure 2. The red lettering represent the process of feeding, sedimentation and filling the sand. Initially, low-concentration tailings slurry is pumped into the empty silo. After a period of settling, the slurry separates into two layers: a supernatant on top and high-concentration tailings at the bottom. Subsequently, more low-concentration slurry is pumped into the silo from the bottom, pushing the supernatant out of the silo. Overflow of the supernatant usually carries a small amount of tailings. This feeding and settling cycle is repeated as needed until the silo is nearly filled with high-concentration tailings, depending on operational requirements.

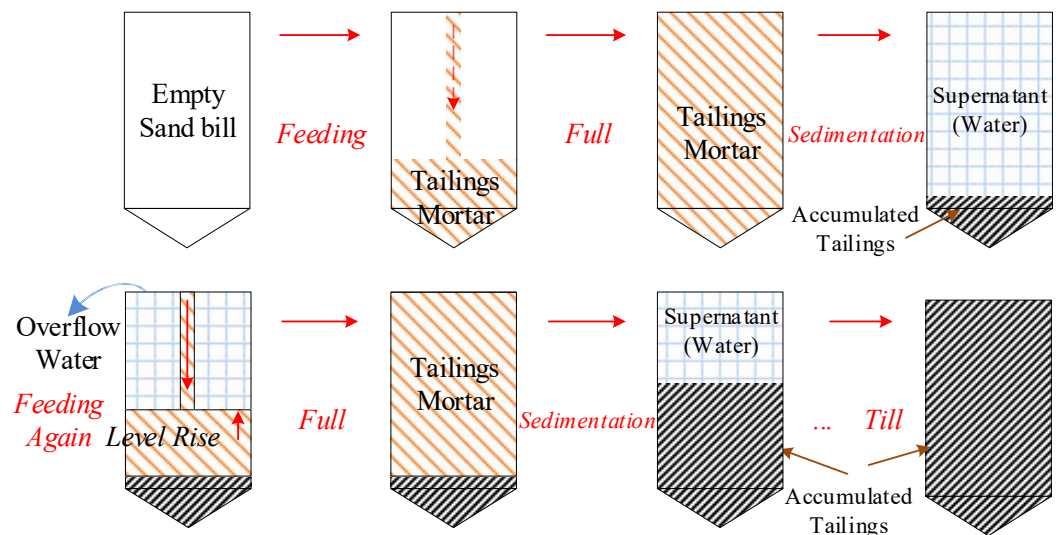


Figure 2. Schematic Diagram of Vertical Sand Silo Feeding and Settling.

The changes in tailings mass within the sand silo during normal operation are illustrated in Figure 3. Initially, the silo is filled with high-concentration tailings, with a mass of MA . As it supports backfilling tasks, the tailings mass inside gradually decreases. When the remaining tailings are deemed insufficient to meet backfilling needs, as stated in the red section, the feeding process is initiated. This process consists of multiple cycles of tailings feeding and settling, leading to intermittent increases in mass within the silo. During these cycles, the silo is unavailable for slurry preparation or backfilling, as stated in the brown section. Once feeding is completed, the silo can again serve backfilling tasks.

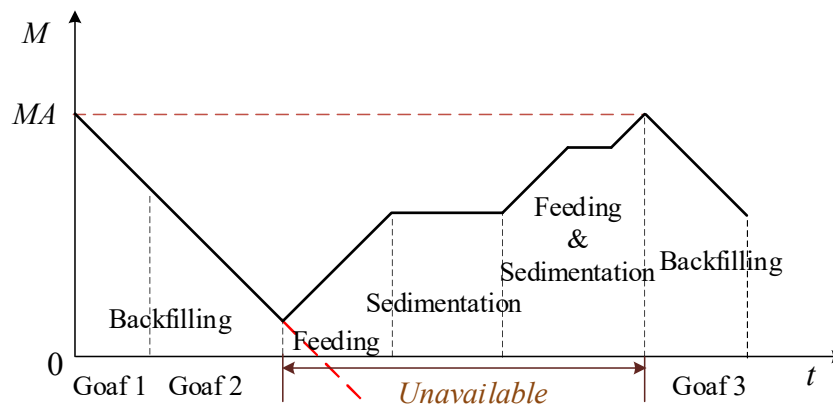


Figure 3. Variation of Tailings Mass and Availability in the Sand Silo.

2.3. Resource Occupancy and Delay

An essential factor in optimizing scheduling is managing resource occupancy. When conflicts arise in equipment allocation, this study prioritizes assigning equipment to the stope ready for filling first. Stopes are sorted by allowed start time, with resources allocated to earlier tasks, while later tasks are scheduled at the next available time slot.

Delays in stope backfilling may result from factors such as equipment reliability issues, sand silo refilling, or conflicting equipment usage schedules. Once backfilling starts, each step must proceed without interruption to prevent incidents such as pipe blockages or bursts caused by slurry solidification. If a delay is anticipated in any step, the start time for backfilling that stope is adjusted, and resources are rescheduled to ensure all required resources are available for each step throughout the process.

2.4. Backfilling Process and Resource Constraints

This study focuses on equipment reliability and preventive maintenance, as well as unavailability due to sand silo feeding and resource occupancy. The resources required for each step in the backfilling process, along with their respective constraints, are shown in Table 1. The backfilling operation consists of four steps: preparation, water flow induction, layered backfilling, and pipeline cleaning. Resources include manpower, water storage, slurry mixing equipment, cementitious material management equipment, and conveying equipment. The abbreviations in the table are explained below. A slash indicates that the process does not require the corresponding resource, so resource constraints are not considered.

Table 1. Resource Constraints for Each Step in the Backfilling Process.

Operation Step	Manpower	Water Storage	Slurry Mixing Equipment	Cementitious Material Management Equipment	Conveying Equipment
Preparation	O	\	\	\	\
Water Flow Induction	O	O, R	\	\	O, R
Layered Backfilling	O	O, R	O, R, S	O, R	O, R
Pipeline Cleaning	O	O, R	\	\	O, R

Abbreviations: O: Occupancy Constraint, R: Reliability Constraint, S: Sand Silo Feeding Constraint, \: Not applicable.

3. Optimization Model Construction

3.1. Model Assumptions, Inputs, and Outputs

The mine backfill scheduling optimization problem under resource constraints can be described as follows: suppose there are A levels in the mining area where mining and backfilling operations are being conducted, with each level containing B_a stopes. Each stope requires C steps. The mining area has D types of resources, with each step requiring at least one type, and the total available resources amount to E_d . Each task has different

resource options, leading to variations in resource occupancy and maintenance, which in turn result in differing delay times.

The model assumptions are as follows:

1. The preceding process for backfilling is mining, and backfilling can only begin once a stope has been mined out. Consequently, each stope has an earliest possible start time for backfilling.
2. At time 0, all slurry mixing equipment is fully stocked with tailings.
3. At any given time, each resource can only serve one backfilling task.
4. Each step may require multiple types of resources, but each step is executed only once and utilizes only one resource from each required type.
5. Backfilling within a stope must proceed continuously; if any resource becomes unavailable, all subsequent steps are delayed.
6. Preparation times between different tasks for the same resource are not considered.
7. The duration of a given backfill task is consistent across all resources.

3.2. Symbols and Definitions

Based on the above assumptions, the symbols used in this model are defined as follows:

Subscripts

- t , Scheduling time index, $t \in (1, 2, \dots, T)$, where T is the total scheduling period?
- a , Level index, $a \in (1, 2, \dots, A)$, where A is the total number of levels in the mining area.
- b , Stope index, $b \in (1, 2, \dots, B_a)$, where B_a is the total number of stopes to be backfilled.
- c , Step index, $c \in (1, 2, \dots, C)$, where C is the maximum number of steps.
- d , Resource type index, $d \in (1, 2, \dots, D)$, where D is the total number of resource types.
- e , Resource unit index, $e \in (1, 2, \dots, E_d)$, where E_d is the total number of units for a specific type of resource.

Parameters

- $BF_{a,b}$, Earliest feasible backfilling time, in hours (h)
- $DT_{a,b,c,d,e}$, Duration of the backfilling task, in hours (h)
- $TB_{a,b,c}$, Tailings consumption for backfilling, in tonnes (t)
- MA_e , Total capacity of tailings held by the slurry mixing equipment, in tonnes (t)
- M_e^t , Mass of tailings in the slurry mixing equipment at time t , in tonnes (t)
- CM_e , Critical mass of tailings in the slurry mixing equipment, in tonnes (t); below this value, additional feeding is required.
- FT_e , Time required for tailings feeding, in hours (h)
- $RT_{d,e}$, Reliability threshold for equipment; maintenance is required if reliability falls below this level
- $MDT_{d,e}$, Duration of equipment maintenance, in hours (h)
- $R_{d,e}^t$, Equipment reliability at time t
- SeT , Equipment service age post-maintenance, in hours (h)
- PN_a , Number of pipelines leading to level a
- FS_0 , Number of primary units for backfilling operations
- N , A large positive integer
- $DeT_{a,b}$, Backfilling delay time, in hours (h)

Decision Variables

- $X_{a,b,c,d,e}^t$, An integer variable, equal to 1 if a resource of type d and unit e is used for the c -th step in stope b at level a at time t ; otherwise, it is 0.
- $Y_{d,e}^t$, An integer variable, equal to 1 if the d -th resource of type e is available at time t ; otherwise, it is 0.
- $Z_{a,b,c}^t$, An integer variable, equal to 1 if the backfilling task begins at time t ; otherwise, it is 0.

Auxiliary Decision Variables

- $RA_{a,b,c,d}$, An integer variable, equal to 1 if a resource of type d can serve the c -th step in stope b at level a ; otherwise, it is 0.
- $ST_{a,b,c}^0$, Expected start time for the backfilling in stope b at level a in hours (h).
- $ST_{a,b,c}$, Actual start time for the c -th step in stope b at level a in hours (h).
- $ET_{a,b,c}$, Expected end time for the c -th step in stope b at level a in hours (h).
- $ET_{a,b,c}^t$, Actual end time for the c -th step in stope b at level a in hours (h).
- $MS_{d,e}^t$, An integer variable, equal to 1 if the backfilling equipment is under maintenance at time t ; otherwise, it is 0.
- S_e^t , An integer variable, equal to 1 if the slurry mixing equipment is undergoing feeding at time t ; otherwise, it is 0.
- $delay, delay_m, delay_t, delay_{on}$, represent total delay time, delay time caused by resource maintenance, sand silo feeding, and equipment occupancy, respectively.

3.3. Optimization Objective

The goal of backfill scheduling is to organize manpower, equipment, and other resources to carry out operations as soon as the backfilling conditions are met in the stope [36]. The benefits are:

1. Minimizing backfill delay time, as the backfilling time for the goaf remains unchanged, the total completion time will be minimized, leading to higher equipment utilization.
2. In the coordinated mining and backfilling mode, timely backfilling enables earlier commencement of the next mining stage, improving overall production efficiency.
3. Prompt backfilling can prevent long-term exposure of the goaf, reducing the risk of roof collapse and side wall failure incidents.

Thus, the optimization goal of the model (Equation (4)) is to minimize the total delay time in backfilling, thereby maximizing production continuity, reducing stope exposure time, and enhancing safety in underground mining.

$$F(x) = \min \sum_{a=1}^A \sum_{b=1}^B (ET_{a,b,c} - BF_{a,b}) = \min \sum_{a=1}^A \sum_{b=1}^B (DeT_{a,b}) \tag{4}$$

3.4. Constraints

The model’s constraints are divided into two categories: backfilling operation constraints and resource availability constraints.

3.4.1. Backfilling Operation Constraints

The following business constraints are implemented to ensure the effective and efficient scheduling of the backfilling process. These constraints govern the logical flow, resource allocation, and timing of various tasks involved in backfilling operations.

1. Each backfilling step c in stope b at level a is performed only once:

$$\sum_{t=1}^T Z_{a,b,c}^t = 1, \forall a, b, c \tag{5}$$

2. Only one resource of each type is selected to serve a specific backfilling task:

$$\sum_{t=1}^T \sum_{e=1}^E X_{a,b,c,d,e}^t = RA_{a,b,c,d}, \forall a, b, c, d \tag{6}$$

3. Earliest feasible backfill time constraint:

$$ST_{a,b,1} \geq BF_{a,b}, \forall a, b \tag{7}$$

- Continuity constraint for backfilling steps, where the start time of the next step is equal to the end time of the current step. When applying this constraint, it is necessary to account for steps that require multiple resource types:

$$ET_{a,b,c} = ST_{a,b,c} + \frac{\sum_{d=1}^D \sum_{e=1}^E \left(DT_{a,b,c,d,e} \cdot \sum_{t=1}^T X_{a,b,c,d,e}^t \right)}{\sum_{d=1}^D \sum_{e=1}^E \sum_{t=1}^T X_{a,b,c,d,e}^t} \tag{8}$$

where:

$$\sum_{d=1}^D \sum_{e=1}^E \sum_{t=1}^T X_{a,b,c,d,e}^t \geq 1ST_{a,b,c+1} = ET_{a,b,c}, \forall a, b, c \in [1, C - 1] \tag{9}$$

3.4.2. Resource Availability Constraints

Equations (11) and (12) correspond to the equipment reliability constraints and maintenance strategies described in Section 2.1. Equations (13) and (14) pertain to the sand silo tailings level assessment and feeding/discharging operational mode discussed in Section 2.2. Equations (10) and (15) correspond to the equipment occupancy constraints described in Section 2.3.

- Pipeline Occupancy Constraint: The number of stopes being backfilled at level a and below must not exceed the number of pipelines leading to level a .

$$\sum_{i=a}^A \sum_{b=1}^B \sum_{c=1}^C Z_{a,b,c}^t \leq PN_a, \forall t \tag{10}$$

- Equipment Reliability Constraint: Before a task begins, the equipment’s reliability at the task’s end must meet the minimum requirement, as indicated by Equation (11).

$$R_{d,e}^{ET_{a,b,c}} \geq RT_{d,e}, \forall e, d \tag{11}$$

If this requirement is not met, as specified in Equation (12), maintenance is required. The resource is marked as unavailable, the task start time is adjusted, and the equipment reliability is updated post-maintenance.

$$\text{if } R_{d,e}^{ET_{a,b,c}} < RT_{d,e}, \text{ then } \begin{cases} MS_{d,e}^{ST_{a,b,c}^0}, \dots, MS_{d,e}^{ST_{a,b,c}^0 + MDT_{d,e}} = 1 \\ ST_{a,b,1} = ST_{a,b,1}^0 + MDT_{d,e} \\ R_{d,e}^{ST_{a,b,1}} = R_{d,e}^{ini} \end{cases} \forall e, d \tag{12}$$

- Slurry Mixing Equipment Feeding Constraint: Before a task begins, the tailings level in the slurry mixing equipment must meet the required amount, as specified by Equation (13).

$$M_e^{ET_{a,b,c}} \geq CM_e, \forall e \tag{13}$$

If this requirement is not satisfied, as indicated in Equation (14), or if the tailings level in the slurry mixing equipment has fallen below the critical value before the task starts, then feeding is initiated. The equipment is marked as unavailable, the backfilling task start time is adjusted, and the tailings level in the slurry mixing equipment is updated.

$$\left. \begin{matrix} M_e^{ST_{a,b,c}^0} \leq CM_e \\ \text{or } M_e^{ET_{a,b,c}} \leq 0 \end{matrix} \right\} \text{ then, } \begin{cases} S_e^{ST_{a,b,c}^0}, \dots, S_e^{ST_{a,b,c}^0 + FT_e} = 1 \\ ST_{a,b,1} = ST_{a,b,1}^0 + FT_e \\ M_e^{ST_{a,b,1}} = MA_e \end{cases} \forall e \tag{14}$$

8. Manpower Resource Constraint: The number of stopes being backfilled at any given time must not exceed the available number of backfilling units.

$$\sum_{d=1}^D \sum_{e=1}^E MS_{d,e}^t \leq MS_0, \forall t \tag{15}$$

3.4.3. Parameter Constraints

9. Equations (16) and (17) establish the assignment relationships between $X_{a,b,c,d,e}^t$ and $Z_{a,b,c}^t$. Both variables are binary, and when $X_{a,b,c,d,e}^t = 1$, the corresponding $Z_{a,b,c}^t$ is also ensured to be 1. Equation (18) defines the assignment relationship between $ST_{a,b,c}$ and $Z_{a,b,c}^t$ where $ST_{a,b,c}$ is equal to the t value for which $Z_{a,b,c}^t = 1$.

$$\sum_{d=1}^D \sum_{e=1}^E X_{a,b,c,d,e}^t \leq N \cdot Z_{a,b,c}^t, \forall a, b, c, t \tag{16}$$

$$\sum_{d=1}^D \sum_{e=1}^E X_{a,b,c,d,e}^t \geq Z_{a,b,c}^t, \forall a, b, c, t \tag{17}$$

$$ST_{a,b,c} = \sum_{t=1}^T t \cdot Z_{a,b,c}^t, \forall a, b, c \tag{18}$$

10. When backfilling equipment is under maintenance or the slurry mixing equipment is in a feeding state, the corresponding resource is unavailable:

$$\text{if } d = 3, S_e^t = 1, \forall e \text{ or } MS_{d,e}^t = 1, \forall d, e, Y_{d,e}^t = 0 \tag{19}$$

4. Algorithm Design

The RCPSP has been proven to be an NP-hard (Non-deterministic Polynomial-time hard) problem [37,38]. The discrete nature of equipment reliability constraints and tailings constraints for slurry mixing equipment further increases the complexity of the solution. Intelligent optimization methods, such as GA, Simulated Annealing (SA), Ant Colony Optimization (ACO), and Particle Swarm Optimization (PSO), are effective for quickly obtaining approximate solutions to large-scale NP-hard problems, offering an advantage in solution efficiency [39]. In this study, the model is implemented using the Python programming language, with GA applied for solving.

4.1. Encoding and Decoding

4.1.1. Encoding Rules

The backfill scheduling problem with multi-resource availability involves assigning the e -th resource of type d to the c backfilling step in stope b at level a , requiring consideration of five dimensions of data. As shown in Equation (20), a chromosome is composed of five dimensions: A, B, C, D , and E , which correspond to level index, stope index, backfilling step index, resource type, and resource unit, respectively. Resource types D (1, 2, 3, 4, 5) represent manpower, water storage, slurry mixing equipment, cementitious material management equipment, and conveying equipment.

$$I = \begin{bmatrix} A \\ B \\ C \\ D \\ E \end{bmatrix} = \begin{bmatrix} 1, 1, 1, \dots, 2, \dots, A \\ 1, 1, 1, \dots, 1, \dots, B_A \\ 1, 2, 2, \dots, 1, \dots, C_{BA} \\ 1, 1, 2, \dots, 2, \dots, D_{CBA} \\ 1, 1, 2, \dots, 1, \dots, E_{DCBA} \end{bmatrix} \tag{20}$$

The logic of the encoding algorithm is illustrated in Figure 4. Based on the above rules, an initial population of individuals is generated with specified population size. The

encoded data includes level information, stope details, backfilling steps, and backfilling resources, forming the initial chromosomes for the algorithm.

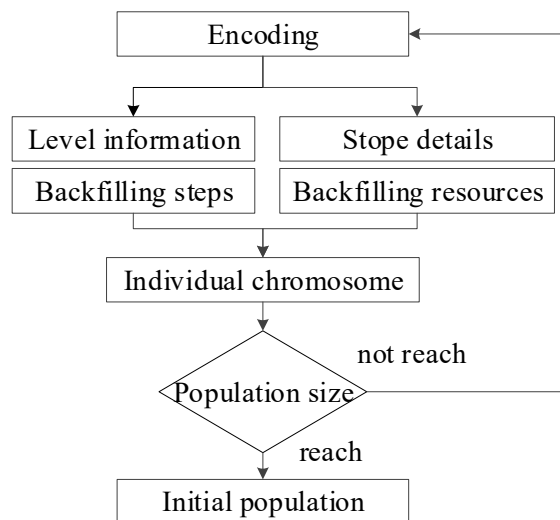


Figure 4. Encoding Algorithm Logic.

The algorithm's solution process must address two key issues: first, that each backfilling task requires multiple resources to operate simultaneously; and second, the timing of when each resource begins servicing the task.

To resolve the first issue, a data dictionary was created to map each backfill task to its required resource types, providing the basis for encoding. Unique identifiers are assigned to differentiate resource types during this process.

For the second issue, precise scheduling times cannot be determined during encoding due to potential delays in the optimization process. To manage this, delay times are calculated and recorded during optimization. In the decoding phase, a detailed schedule—incorporating timing—is generated using these delay times and the earliest possible start time.

4.1.2. Decoding Algorithm

The logic of the decoding algorithm is illustrated in Figure 5.

The detailed decoding steps are as follows:

1. With known level indices, stopes, backfilling step durations, allowed start times, and tailings consumption, stopes are sorted based on the allowed start time.
2. According to Equation (3), calculate the resource reliability R after completing the c -th step in stope b at level a . If $R_{d,e}^{ET_{a,b,c}} \geq RT_{d,e}$, the resource does not require maintenance. Otherwise, maintenance is performed, rendering the resource unavailable. A maintenance record is created, and the R is reset. The delay caused by maintenance is equal to the maintenance duration, $delay_m = MDT_{d,e}$, and the resource's service age is updated accordingly.
3. Check whether the tailings weight can meet the requirements for backfilling stope b at level a . If $M_e^{ET_{a,b,c}} \geq CM$, the equipment has sufficient tailings and no additional feeding is needed. Otherwise, feeding is performed, create a feeding record, and update the new tailings level. The delay caused by insufficient tailings is equal to the feeding time, $delay_t = FT_e$.
4. Calculate the occupancy times for all resources required to determine whether each resource is within its available time. If yes, no further action is needed; otherwise, calculate the delay caused by resource occupancy, $delay_on$.
5. Calculate the overall delay for backfilling using Equation (21). The actual start time is obtained by adding this delay to the allowed start time of the stope. Determine the

timing for each task, create the backfilling schedule for the stope, and update resource occupancy accordingly.

$$DeT_{ab} = delay_{on} + delay_m + delay_t \tag{21}$$

6. Return to Step 2 and proceed with calculations for the next stope until scheduling plans are completed for all stopes.
7. Calculate the total delay across all stopes, using it as the fitness value for the GA. Return the detailed schedule, fitness value, maintenance records, and feeding records.

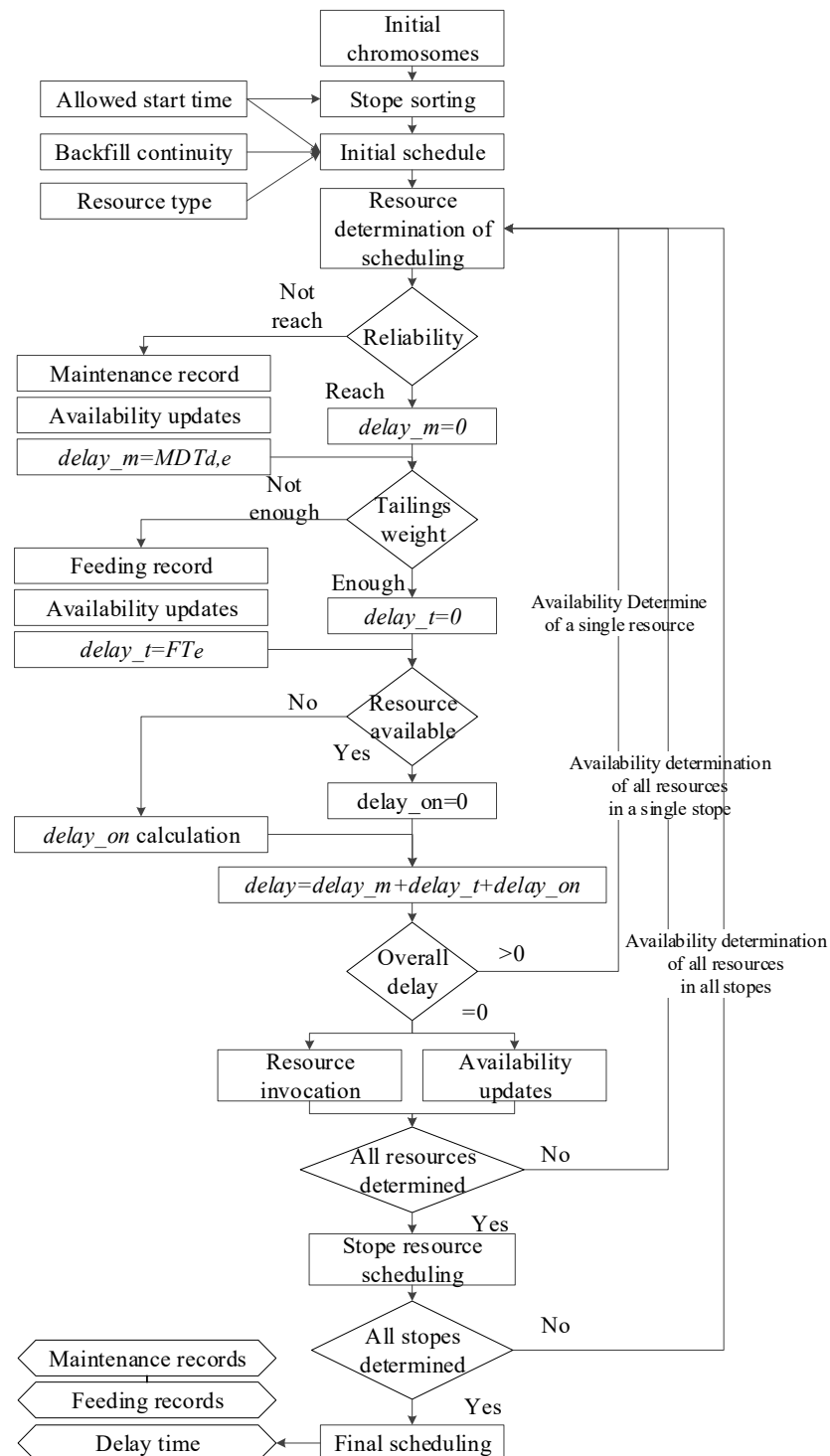


Figure 5. Decoding Algorithm Logic.

4.2. Execution Process of the GA

The execution process of the GA includes population initialization, evaluation and selection, crossover and mutation, and fitness calculation. The steps for implementing the GA in this model are as follows:

1. Define parameters such as population size, number of iterations, and mutation probability.
2. Initialize the first generation of the population according to the encoding rules. Calculate fitness values through decoding, copy the best individual to replace the worst individual to ensure elitism, and update the global best individual. Elitism ensures that the best individual in each generation is passed to the next generation.
3. Select two parent individuals using a roulette-wheel selection method and apply two-point crossover to generate offspring. Roulette wheel selection determines the probability of an individual being chosen as a parent based on its fitness. Two-point crossover selects two crossover points in two parent genes and exchanges sequences to produce new individuals.
4. Define mutation rules, allowing mutation only within the same resource type. Mutate resource numbers according to the mutation probability to create new offspring. Mutation randomly alters an individual's genes to increase diversity and prevent premature convergence.
5. Decode the new offspring and calculate their fitness values, retaining the two best individuals and updating the global best.
6. Repeat steps (3), (4), and (5) until the specified number of iterations is reached.
7. Return the global best individual.

In a simple GA, suppose we have individuals and fitness values as shown in Table 2:

Table 2. Example gene of GA.

Individual	Gene	Fitness
1	101010	20
2	110011	30
3	111000	50

Execute the following steps:

- Selection: Use the roulette wheel selection method to select two individuals, such as individual 2 and individual 3.
- Crossover: After performing the two-point crossover, two new offspring individuals are generated, such as the new individuals "110000" and "111011" produced by the crossover between individual 2 and individual 3.
- Mutation: Apply mutation to the offspring "110000", which could change to "110001".
- Elitism: Retain the current best individual (for example, the individual with a fitness of 50) and directly pass it to the next generation.

The individuals after executing the GA are: "110001", "111011", and "111000".

The search logic of the algorithm involves assigning resources of the same type but with different identifiers to tasks. To ensure that all generated solutions are valid, crossover and mutation operations are applied exclusively to the *E* dimension of the chromosome. Crossover is permitted only when the *D* values of the two chromosomes are identical, indicating the use of the same type of equipment. Similarly, the mutation range is restricted to the same category of resources. For instance, if the *E* value is 5, representing human resources with an identifier range of (1, 6) the mutation is confined to this range.

5. Case Study, Results Analysis, and Discussion

To verify the effectiveness of the model and algorithm, an empirical analysis is conducted using production data from a large underground metal mine in Shandong, China. The mine operates at a production scale of 8000 t/d and employs an upward layered

backfilling method. The backfill structure is divided into two layers vertically, with five sequential backfilling steps: preliminary preparation, water flow induction, bottom filling, top filling, and pipeline cleaning, where C is set to 5.

5.1. Case Data and Inputs

The mine establishes a monthly backfilling plan, with adjustments and optimizations approximately every ten days. During a specific optimization instance, 27 stopes in 11 levels were scheduled for backfilling; detailed stope information is provided in Appendix A. The backfilling station includes six tailings silos, each equipped with corresponding mixing facilities, collectively forming a slurry mixing system. Three backfilling teams are available, each capable of handling two tasks simultaneously. Additionally, there are two water storage units and two cementitious material silos, each independently able to meet the water and material demands of all the slurry mixing systems. A total of six pipelines connect to the underground backfill main network.

The equipment reliability data is sourced from the ledger and management system of the backfilling center at the mine, covering equipment operation and failure data since 2020. The dataset includes various metrics such as equipment usage time, failure records, maintenance history, and more, encompassing different types of equipment and operating conditions. The Pareto principle was applied to analyze equipment failure modes. The backfilling station at the case has been in service for several years, with equipment now in the wear-out phase, corresponding to the third stage of the bathtub curve, where $\beta > 1$. This process follows a Non-homogeneous Poisson Process (NHPP). The equipment failure rate function adheres to a Weibull distribution, with fitted parameters for the Weibull function shown in Table 3. The primary backfilling units remain continuously available, with a reliability of 1. When the model is applied to other mines, it will need to be adapted according to actual data and select different failure functions based on the specific failure modes observed.

Table 3. Reliability Parameters for Backfilling Equipment.

Type	β	η	r	Service Age (h)	D	E
Manpower	\	\	\	\	1	1, 2, 3, 4, 5, 6
Water tank	2	1920	0	550, 550, 550, 420, 420, 420	2	6, 7, 8, 9, 10, 11
Pulping & mixing	2	969	0	490, 210, 430, 150, 480, 270	3	12, 13, 14, 15, 16, 17
Cementitious material	2	1983	0	460, 460, 460, 390, 390, 390	4	18, 19, 20, 21, 22, 23
Slurry conveying	2	2064	0	480, 510, 530, 550, 570, 590	5	24, 25, 26, 27, 28, 29

As shown in Table 3, when the value range of E is (1, 6), it represents human resources, and its reliability is set to 1 by default, so no other parameters need to be assigned.

Calculating the reliability of the water tank and cementitious material management equipment is relatively complex, as these two systems operate in parallel. The combined reliability of the parallel configuration is determined using Equation (22). This parallel setup is then represented as six virtual units with uniform reliability, with their service age cumulatively tracked across tasks.

$$R_p(t) = 1 - [1 - R_1(t)] \cdot [1 - R_2(t)] \tag{22}$$

In summary, additional data required for the model are listed in Table 4, including the values or ranges for A, B, C, D, and E; the tailings capacity and feeding time for the slurry mixing equipment; and the equipment reliability threshold.

Table 4. Additional Input Data for the Model.

Parameter	Value	Parameter	Value
<i>MA</i> (t)	1424	<i>A</i>	11
<i>FT</i> (h)	10	<i>B</i>	1–3
<i>RT</i>	0.8	<i>C</i>	5
<i>MDT</i> (h)	12	<i>D</i>	5
<i>SeT</i> (h)	80	<i>E</i>	1–30
<i>FS</i> ₀	6	<i>N</i>	10 ⁵

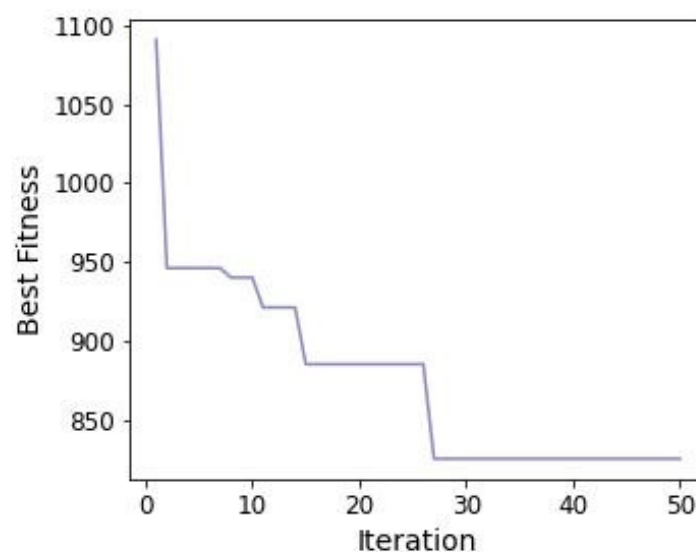
5.2. Optimization Results

The model is constructed using Python on the Anaconda platform, and the computations are performed on a Lenovo Thinkpad notebook equipped with an Intel Core i7-8550 processor, that was purchased in Shanghai, China. The parameters of the GA, such as crossover rate, mutation rate, and population size, significantly affect the solving speed and efficiency.

A higher crossover rate and mutation rate can accelerate convergence but may reduce the diversity of solutions, potentially leading to the loss of the optimal solution. Conversely, when the crossover rate is too low, the convergence speed decreases, and the probability of obtaining suboptimal solutions increases. However, under the elitism strategy, the loss of the optimal solution does not occur. To reduce computational intensity and the number of iterations, this case study adopts relatively high crossover and mutation rates, both set at 0.2.

A larger population size requires more computational resources and time but provides a broader range of solutions. In this case study, multiple simulations were conducted with the same number of iterations (50). When the population size was 20, only 2 out of 10 simulations achieved an approximate minimum value (825 h). As the population size increased, the number of times the optimal fitness value was achieved also increased. When the population size reached 50, all 10 simulations achieved the optimal fitness value.

Regarding computation time and efficiency, the time per iteration varied between 6 and 9 min. However, the number of iterations required to reach the optimal fitness value varied. Subsequently, a set of data was randomly selected to represent the iterative process. Figure 6 shows the trend of fitness value changes during the iterations, displaying a gradient descent and reaching the minimum value at the 27th generation.

**Figure 6.** GA Iteration Chart.

The model solution results are shown in Table 5, presenting the start, end, and delay times for slope backfilling. Due to space constraints, only data for 2 out of the 5 dimensions is displayed in the table. Using the first slope in the first level as an example, the resource allocation for each backfilling step is detailed in Table 6.

Table 5. Model Solution Results.

Level/A	Slope/B	Start (h)	End (h)	Delay (h)
1	1	0	13	0
1	2	48	59	0
2	1	34	48	10
2	2	34	49	10
2	3	14	33	14
3	1	61	79	13
3	2	10	32	10
3	3	51	71	51
4	1	80	102	32
4	2	43	59	19
4	3	94	112	70
5	1	112	135	88
5	2	96	111	0
6	1	130	150	10
7	1	41	63	41
7	2	73	96	25
7	3	152	173	56
7	4	113	137	65
8	1	61	77	13
8	2	175	191	31
8	3	103	125	55
9	1	147	166	75
9	2	158	182	14
10	1	193	212	73
10	2	88	101	16
11	1	121	138	25
11	2	129	146	9

Table 6. Backfilling Resource Allocation (Example: First Slope (B) in the First Level).

Level/A	Slope/B	Step/C	Type/D	No./E	Start (h)	End (h)
1	1	1	1	5	0	8
1	1	2	1	5	8	8.5
1	1	2	2	10	8	8.5
1	1	2	5	28	8	8.5
1	1	3	1	5	8.5	11.5
1	1	3	2	10	8.5	11.5
1	1	3	3	16	8.5	11.5
1	1	3	4	19	8.5	11.5
1	1	3	5	28	8.5	11.5
1	1	4	1	5	11.5	12.5
1	1	4	2	10	11.5	12.5
1	1	4	3	16	11.5	12.5
1	1	4	4	19	11.5	12.5
1	1	4	5	28	11.5	12.5
1	1	5	1	5	12.5	13
1	1	5	2	10	12.5	13
1	1	5	5	28	12.5	13

Table 6 provides a clear view of the resource IDs (E) and types (D) used in each backfilling step (C), along with the start and end times for resource allocation.

Figure 7 illustrates the optimal Gantt chart for the stope backfilling schedule. The horizontal axis denotes the scheduling time in hours, while the vertical axis displays the level numbers and stope identification codes. Five different colors are used in the chart to distinguish the backfilling steps, with each color representing a specific operation phase.

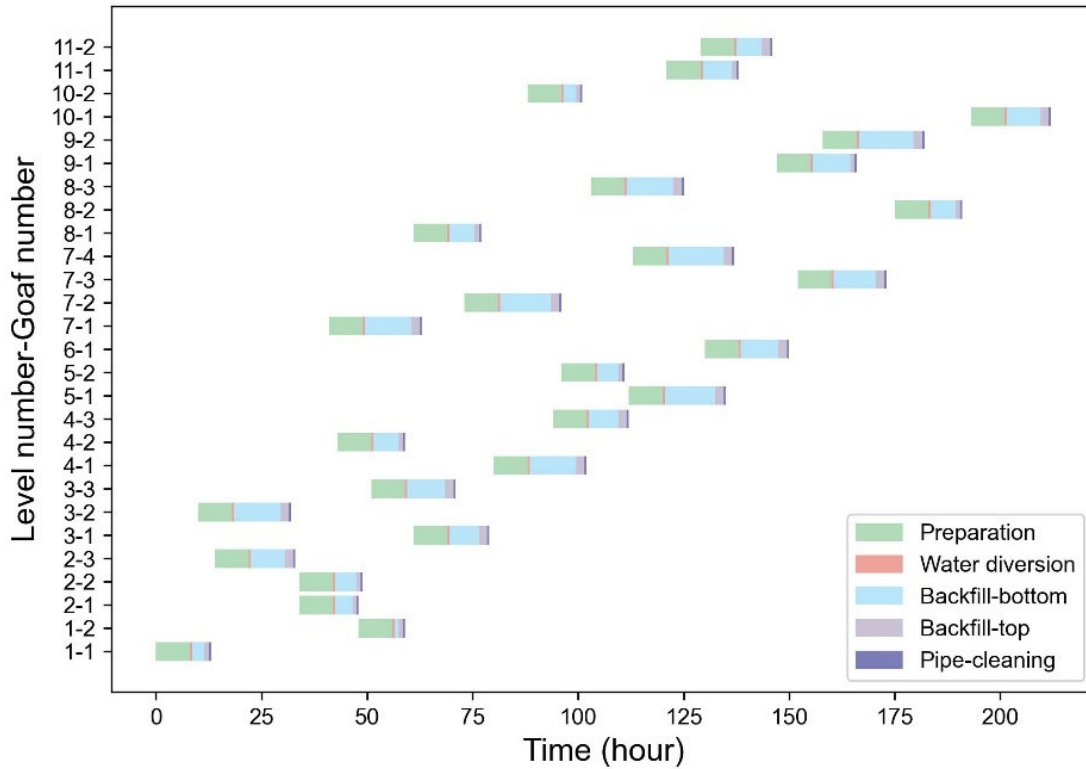


Figure 7. Stope Backfilling Schedule.

Figure 8 demonstrates the utilization status of five backfilling resources, where the horizontal axis represents time and the vertical axis indicates resource types (resource codes are detailed in Table 2). As in the case description, each number in PM and SC represents a resource. The data in the box represents the level No.- stope No. Seven colors are employed in the chart: the first five colors correspond to the basic backfilling resources, while the sixth color (yellow) indicates the sand feeding status of the slurry mixing equipment, and the seventh color (purple) represents equipment maintenance status. During this scheduling period, 13 sand feeding operations and 2 equipment maintenance sessions were recorded. Notably, human resources, water tanks, and cementitious material management equipment can simultaneously serve multiple backfilling processes; thus, their specific service allocation to individual stops is not marked in the figure.

As shown in Figure 8, pumping equipment PM-5 exhibits the lowest utilization rate, primarily due to its extended service age. The frequent maintenance requirements of this equipment would increase scheduling delays and consequently raise the fitness value. Regarding slurry transportation equipment, pipelines SC-3 and SC-4 show significantly higher utilization rates compared to other facilities. This can be attributed to their dedicated function in serving deeper levels, as the backfilling slurry for deep stopes can only be transported through these two specific pipeline routes.

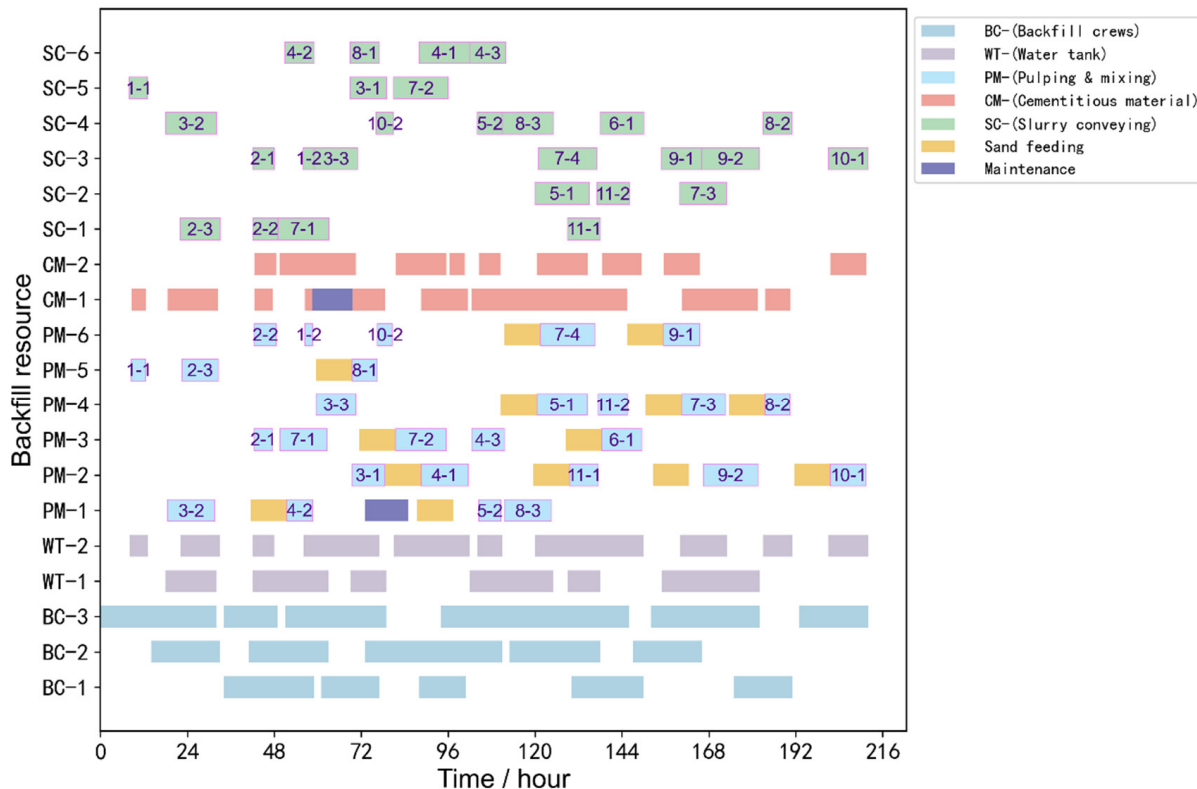


Figure 8. Resource Allocation Distribution.

5.3. Advantages over Traditional Mode

This model implements precise scheduling by comprehensively considering the operational characteristics and reliability of slurry mixing equipment. Compared to the current ‘one-operating-one-standby’ mode used in mines, where only 50% of total resources are available at any given time, this model optimizes the synergistic utilization of all system resources, thereby significantly improving operational efficiency. Table 7 presents a comparative summary of scheduling results between the traditional mode and the optimized solution.

Table 7. Backfilling Resource Allocation (Example: First Stope in the First Level).

	Traditional	Optimization
Makespan (h)	267	212
Utilization	31.07%	39.13%
Total delay (h)	1568	825

Compared to the traditional model, the optimized solution offers significant advantages, primarily in the following areas:

1. Completion time was reduced by 20.6%, from 267 h to 212 h.
2. Resource utilization increased by 8 percentage points, from 31.07% to 39.13%.
3. Total delay time decreased by 47.4%, from 1568 h to 825 h. This reduction significantly minimizes goaf exposure time, allowing for more timely ground pressure management and reducing the risk of ground pressure incidents.

5.4. Limitation and Future Research

Despite the model’s effectiveness in the current mining context, its generalizability to diverse equipment types and complex operational scenarios requires further investigation.

The model validation was primarily conducted under specific operational conditions, which may limit its broader applicability.

Future research directions include:

1. Extending the model to accommodate diverse equipment types and environmental factors, particularly non-linear failure modes.
2. Investigating the model's real-time implementation in large-scale mining operations, with emphasis on computational efficiency.
3. Integrating advanced technologies such as artificial intelligence and big data analytics to enhance the model's adaptability and robustness in dynamic mining environments.

The proposed extensions would significantly advance the practical application of backfill scheduling optimization in modern mining operations.

6. Conclusions

This study develops a scheduling optimization model for backfilling operations under resource constraints, addressing the complex requirements of coordinating multiple resources, sequential steps, stopes, and specific process-related needs. To achieve effective scheduling, a tailored algorithm has been designed to solve the model, and its effectiveness has been validated through application to a case study mine, optimizing the assignment of backfilling personnel, equipment, and tasks. Comparative analysis with conventional scheduling approaches confirms the model's effectiveness. The main findings are as follows:

1. **Resource-Constrained Scheduling Optimization Model:** This study systematically identifies the various resource requirements in mine backfilling processes and examines operational procedures when resources are unavailable. By incorporating constraints on resource availability and setting total backfilling delay time as the optimization objective, the model provides a comprehensive approach to scheduling that accounts for multiple resource limitations.
2. **Heuristic Solution Algorithm for Complex Processes:** Given the NP-hard nature of the problem, a heuristic algorithm has been applied, featuring encoding methods adapted to process constraints and decoding methods aligned with resource limitations. The algorithm calculates delay times as fitness values and integrates specific procedures for managing resource unavailability, ensuring a structured and efficient solution process.
3. **Model Validation and Performance Analysis:** Detailed data processing has been conducted for the case study mine, producing a precise scheduling solution that identifies start and end times for each task across various resources. Compared to the traditional model, the optimized scheduling solution shows clear advantages, with a 20.6% reduction in completion time, an 8-percentage point increase in resource utilization, and a 47.4% reduction in total backfilling delay time.

In conclusion, this study presents a novel optimization model for mine backfill scheduling, along with its solution methodology and validation through a real-world case study. The model demonstrates both theoretical significance and practical value in mining operations. By implementing intelligent scheduling optimization in mine backfilling, the model not only enhances production efficiency and underground mining safety but also advances mining intelligentization. The model's capability for dynamic decision-making and optimal resource allocation provides valuable support for intelligent mining operations, particularly in addressing complex scheduling challenges in modern mining environments.

Author Contributions: Methodology, G.L.; Model, J.H.; Validation, Y.L.; Resources, C.F., C.T. and P.W.; Result analysis, J.H. and Y.L.; Writing—original draft, Y.L.; Writing—review and editing, G.L. and J.H.; Visualization, Y.L.; Supervision, G.L. All authors have read and agreed to the published version of the manuscript.

Funding: This research was funded by the National Key Research and Development Program of China–2023 Key Special Project (No. 2023YFC2907403), the National Natural Science Foundation of China (No. 52404161), and the China Scholarship Council (202206460036).

Data Availability Statement: Data are contained within the article.

Acknowledgments: The authors would like to express their sincere gratitude to Justin, Qixuan Song, and Chu Chu for their valuable insights and constructive suggestions on the solution methodology. The authors also appreciate the anonymous reviewers for their helpful comments that improved the quality of this paper.

Conflicts of Interest: Panzhi Wang is employee of Jiaojia Gold Mine, Shandong Gold Group Mining (Laizhou) Co., Ltd., Yantai, China. The paper reflects the views of the scientists and not the company.

Appendix A. Input Data, Stopes Information

No.	Level/A	Goaf/B	Earliest Time/BF (h)	Tailings/TB (t)		Backfill Duration/DT (h)				
				Bottom	Top	1	2	3	4	5
1	1	1	0	289.5	47.8	8	0.5	3	1	0.5
2	1	2	48	90.1	11	8	0.5	1	1	0.5
3	2	1	24	349.8	33	8	0.5	4	1	0.5
4	2	2	24	440.4	75.7	8	0.5	5	1	0.5
5	2	3	0	778.1	96.8	8	0.5	8	2	0.5
6	3	1	48	778.1	117	8	0.5	7	2	0.5
7	3	2	0	981.8	108.4	8	0.5	11	2	0.5
8	3	3	0	852.4	115.3	8	0.5	9	2	0.5
9	4	1	48	1018.3	121	8	0.5	11	2	0.5
10	4	2	24	550.3	65.1	8	0.5	6	1	0.5
11	4	3	24	646.6	96.8	8	0.5	7	2	0.5
12	5	1	24	1106.3	134.7	8	0.5	12	2	0.5
13	5	2	96	476.3	57.3	8	0.5	5	1	0.5
14	6	1	120	879.2	113.3	8	0.5	9	2	0.5
15	7	1	0	1093	116.6	8	0.5	11	2	0.5
16	7	2	48	1129.4	120.2	8	0.5	12	2	0.5
17	7	3	96	1087.3	112	8	0.5	10	2	0.5
18	7	4	48	1044.7	126.8	8	0.5	13	2	0.5
19	8	1	48	536.5	73.3	8	0.5	6	1	0.5
20	8	2	144	559.8	71.6	8	0.5	6	1	0.5
21	8	3	48	1051.2	129.1	8	0.5	11	2	0.5
22	9	1	72	833.5	79.5	8	0.5	9	1	0.5
23	9	2	144	1278.6	143.8	8	0.5	13	2	0.5
24	10	1	120	742.4	119.6	8	0.5	8	2	0.5
25	10	2	72	251.8	30.7	8	0.5	3	1	0.5
26	11	1	96	651.8	61.4	8	0.5	7	1	0.5
27	11	2	120	536.4	92.1	8	0.5	6	2	0.5

References

1. Behera, S.K.; Mishra, D.P.; Singh, P.; Mishra, K.; Mandal, S.K.; Ghosh, C.N.; Kumar, R.; Mandal, P.K. Utilization of mill tailings, fly ash and slag as mine paste backfill material: Review and future perspective. *Constr. Build. Mater.* **2021**, *309*, 125120. [\[CrossRef\]](#)
2. Kasap, T.; Yilmaz, E.; Sari, M. Physico-chemical and micro-structural behavior of cemented mine backfill: Effect of pH in dam tailings. *J. Environ. Manag.* **2022**, *314*, 115034. [\[CrossRef\]](#) [\[PubMed\]](#)
3. Guo, M.; Tan, Y.; Chen, D.; Song, W.; Cao, S. Optimization and Stability of the Bottom Structure Parameters of the Deep Sublevel Stope with Delayed Backfilling. *Minerals* **2022**, *12*, 709. [\[CrossRef\]](#)
4. Zhang, C.; Taheri, A.; Du, C.; Xia, W.; Tan, Y. Mechanical Characteristics and Macro–Microscopic Response Mechanisms of Cemented Paste Backfill under Different Curing Temperatures. *Minerals* **2024**, *14*, 433. [\[CrossRef\]](#)
5. Ji, X.; Gu, X.; Wang, Z.; Xu, S.; Jiang, H.; Yilmaz, E. Admixture Effects on the Rheological/Mechanical Behavior and Micro-Structure Evolution of Alkali-Activated Slag Backfills. *Minerals* **2022**, *13*, 30. [\[CrossRef\]](#)
6. Wang, B.; Gan, S.; Yang, L.; Zhao, Z.; Wei, Z.; Wang, J. Additivity Effect on Properties of Cemented Ultra-Fine Tailings Backfill Containing Sodium Silicate and Calcium Chloride. *Minerals* **2024**, *14*, 154. [\[CrossRef\]](#)
7. Wang, Z.; Jiang, H.; Fu, Y.; Ma, Z.; Wang, X. Calcined alunite-modified alkali-sulphate-activated slag as a novel binder for high-performance cemented paste backfill. *J. Build. Eng.* **2024**, *91*, 109687. [\[CrossRef\]](#)
8. Chen, X.; Guo, L.; Zhou, Y.; Xu, W.; Zhao, Y. Remediation of grassland subsidence and reduction of land occupation with tailings backfill technology: A case study of lead-zinc mine in Inner Mongolia, China. *Front. Environ. Sci.* **2023**, *11*, 1183945. [\[CrossRef\]](#)

9. Lu, H.; Qi, C.; Chen, Q.; Gan, D.; Xue, Z.; Hu, Y. A new procedure for recycling waste tailings as cemented paste backfill to underground stopes and open pits. *J. Clean. Prod.* **2018**, *188*, 601–612. [[CrossRef](#)]
10. Mashifana, T.; Sithole, T. Clean production of sustainable backfill material from waste gold tailings and slag. *J. Clean. Prod.* **2021**, *308*, 127357. [[CrossRef](#)]
11. Qi, C.; Fourie, A. Cemented paste backfill for mineral tailings management: Review and future perspectives. *Miner. Eng.* **2019**, *144*, 106025. [[CrossRef](#)]
12. Liu, Y.; Li, G.; Hou, J.; Guo, G.; Pan, D.; Yu, Q. An Underground Mine Safety-Oriented Optimization Model for Mine Tailings Backfill Scheduling Considering Multi-Process and Multi-Cycle Issues. *Minerals* **2023**, *13*, 1409. [[CrossRef](#)]
13. Liu, K.; Mei, B.; Li, Q.; Sun, S.; Zhang, Q. Collaborative Production Planning Based on an Intelligent Unmanned Mining System for Open-Pit Mines in the Industry 4.0 Era. *Machines* **2024**, *12*, 419. [[CrossRef](#)]
14. Wu, A.; Wang, Y.; Ruan, Z.E.; Xiao, B.; Wang, J.; Wang, L. Key theory and technology of cemented paste backfill for green mining of metal mines. *Green Smart Min. Eng.* **2024**, *1*, 27–39. [[CrossRef](#)]
15. Wang, Z.; Wu, A.; Ruan, Z.; Bürger, R.; Wang, S.; Mo, Y. Flocculation behavior, mechanics, and optimization of tailings based on multi-objective: Insight into the concentration and time-dependent floc size. *Powder Technol.* **2024**, *439*, 119718. [[CrossRef](#)]
16. Löw, J.; Abrahamsson, L.; Johansson, J. Mining 4.0—The Impact of New Technology from a Work Place Perspective. *Min. Metall. Explor.* **2019**, *36*, 701–707. [[CrossRef](#)]
17. Zhironkina, O.; Zhironkin, S. Technological and Intellectual Transition to Mining 4.0: A Review. *Energies* **2023**, *16*, 1427. [[CrossRef](#)]
18. Hou, J.; Wang, H.; Li, G.; Sheng, B.; Wang, Q. Multistage dynamic optimisation of ore flow for underground metal mines. *Int. J. Min. Reclam. Environ.* **2024**, *38*, 407–423. [[CrossRef](#)]
19. Jiang, S.; Lian, M.; Lu, C.; Gu, Q.; Ruan, S.; Xie, X. Ensemble Prediction Algorithm of Anomaly Monitoring Based on Big Data Analysis Platform of Open-Pit Mine Slope. *Complexity* **2018**, *2018*, 1–13. [[CrossRef](#)]
20. Xu, X.-c.; Gu, X.-w.; Wang, Q.; Gao, X.-w.; Liu, J.-p.; Wang, Z.-k.; Wang, X.-h. Production scheduling optimization considering ecological costs for open pit metal mines. *J. Clean. Prod.* **2018**, *180*, 210–221. [[CrossRef](#)]
21. Johnson, S.M. Optimal two- and three-stage production schedules with setup times included. *Nav. Res. Logist. Q.* **1954**, *1*, 61–68. [[CrossRef](#)]
22. Brucker, P.; Schlie, R. Job-shop scheduling with multi-purpose machines. *Computing* **1990**, *45*, 369–375. [[CrossRef](#)]
23. Gong, G.; Chiong, R.; Deng, Q.; Gong, X. A hybrid artificial bee colony algorithm for flexible job shop scheduling with worker flexibility. *Int. J. Prod. Res.* **2020**, *58*, 4406–4420. [[CrossRef](#)]
24. Soltani Khaboushan, A.; Osanloo, M.; Esfahanipour, A. Optimization of open pit to underground transition depth: An idea for reducing waste rock contamination while maximizing economic benefits. *J. Clean. Prod.* **2020**, *277*, 123530. [[CrossRef](#)]
25. Upadhyay, S.P.; Askari-Nasab, H. Simulation and optimization approach for uncertainty-based short-term planning in open pit mines. *Int. J. Min. Sci. Technol.* **2018**, *28*, 153–166. [[CrossRef](#)]
26. Vaziri, V.; Sayadi, A.R.; Mousavi, A.; Parbhakar-Fox, A.; Monjezi, M. Mathematical modeling for optimized mine waste rock disposal: Establishing more effective acid rock drainage management. *J. Clean. Prod.* **2021**, *288*, 125124. [[CrossRef](#)]
27. Guo, L.; Funari, V.; Li, M. Editorial: Advances in sustainable mine tailings management. *Front. Earth Sci.* **2023**, *11*, 1269955. [[CrossRef](#)]
28. Kou, Y.; Liu, Y.; Li, G.; Hou, J.; Luan, L.; Wang, H.; Guo, L. Design and Implementation of an Integrated Management System for Backfill Experimental Data. *Adv. Civ. Eng.* **2022**, *2022*, 1–9. [[CrossRef](#)]
29. Bahroun, Z.; Tanash, M.; As'ad, R.; Alnajjar, M. Artificial Intelligence Applications in Project Scheduling: A Systematic Review, Bibliometric Analysis, and Prospects for Future Research. *Manag. Syst. Prod. Eng.* **2023**, *31*, 144–161. [[CrossRef](#)]
30. Chimunhu, P.; Topal, E.; Ajak, A.D.; Asad, W. A review of machine learning applications for underground mine planning and scheduling. *Resour. Policy* **2022**, *77*, 102693. [[CrossRef](#)]
31. Ding, H.; Zhuang, C.; Liu, J. Extensions of the resource-constrained project scheduling problem. *Autom. Constr.* **2023**, *153*, 104958. [[CrossRef](#)]
32. Nesbitt, P.; Blake, L.R.; Lamas, P.; Goycoolea, M.; Pagnoncelli, B.K.; Newman, A.; Brickey, A. Underground mine scheduling under uncertainty. *Eur. J. Oper. Res.* **2021**, *294*, 340–352. [[CrossRef](#)]
33. Johnson, R.T.J. An Algorithm for the Resource Constrained Project Scheduling Problem. Ph.D. Thesis, Massachusetts Institute of Technology, Cambridge, MA, USA, 1967.
34. Yin, S.; Shao, Y.; Wu, A.; Wang, H.; Liu, X.; Wang, Y. A systematic review of paste technology in metal mines for cleaner production in China. *J. Clean. Prod.* **2020**, *247*, 119590. [[CrossRef](#)]
35. Qi, C.; Fourie, A.; Chen, Q.; Zhang, Q. A strength prediction model using artificial intelligence for recycling waste tailings as cemented paste backfill. *J. Clean. Prod.* **2018**, *183*, 566–578. [[CrossRef](#)]
36. Huang, S.; Li, G.; Ben-Awuah, E.; Afum, B.O.; Hu, N. A robust mixed integer linear programming framework for underground cut-and-fill mining production scheduling. *Int. J. Min. Reclam. Environ.* **2019**, *34*, 397–414. [[CrossRef](#)]
37. Golab, A.; Gooya, E.S.; Falou, A.A.; Cabon, M. Review of conventional metaheuristic techniques for resource-constrained project scheduling problem. *J. Proj. Manag.* **2022**, *7*, 95–110. [[CrossRef](#)]

-
38. Hartmann, S.; Briskorn, D. A survey of variants and extensions of the resource-constrained project scheduling problem. *Eur. J. Oper. Res.* **2010**, *207*, 1–14. [[CrossRef](#)]
 39. Pellerin, R.; Perrier, N.; Berthaut, F. A survey of hybrid metaheuristics for the resource-constrained project scheduling problem. *Eur. J. Oper. Res.* **2020**, *280*, 395–416. [[CrossRef](#)]

Disclaimer/Publisher’s Note: The statements, opinions and data contained in all publications are solely those of the individual author(s) and contributor(s) and not of MDPI and/or the editor(s). MDPI and/or the editor(s) disclaim responsibility for any injury to people or property resulting from any ideas, methods, instructions or products referred to in the content.